Biosorption studies on the removal of heavy metals Copper and Chromium using chitosan nanoparticles based biocomposite

R. Sasirekha[1], G. Sivasankari[2], S. Gunasekaran[3], N. Manimaran[4], K. Santhanalakshmi[5] and Thandapani Gomathi[1]*

[1,1*]PG and Research Department of Chemistry, D.K.M. College for Women (Autonomous), Affiliated to Thiruvalluvar University, Vellore-632001, Tamil Nadu, India

[2] PG Department of Chemistry, Cauvery College for Women (Autonomous), Affiliated to Bharathidasan University, Trichy–620018, Tamil Nadu, India

[3]Department of Chemistry, Paavendhar College of Arts and Science, Affiliated to Periyar University M.V. South – 636121, Attur, Salem

[4]School of Chemistry, Bharathidasan University, Trichy – 620024, Tamil Nadu, India

[5]Department of Humanities and Sciences, IFET College of Engineering (Autonomous), Villupuram, Tamil Nadu, India

drgoms1@gmail.com

Abstract

The objective of the current work was to assess the efficacy of biocomposite materials made of chitosan nanoparticles (CS-NPs), alginate (AL), and hydroxyapatite (HAP) for the removal of copper (Cu) and chromium (Cr) ions. These dangerous heavy metals are removed using CS-NPs/AL/HAP ternary biocomposite, which has NH_2, COO^- and OH functional groups. Through FTIR and XRD investigations, the formation of the biocomposite material was verified. SEM analysis results showed the surface of the biocomposite was rough in nature. Batch adsorption studies were conducted and the results demonstrated that Cu^{2+} and Cr^{6+} ion removal was pH-dependent (pH 5). The experimental results were analyzed using Langmuir and Freundlich isotherm models. Based on the R^2 values, it was demonstrated that the Freundlich isotherm (R^2 = 0.9933 for Cu^{2+} and 0.9979 for Cr^{6+}) rather than the Langmuir isotherm (R^2 = 0.9273 for Cu^{2+} and 0.9051 Cr^{6+}) best describes the adsorption process. Additionally, the sorption capacity of Cu^{2+} and Cr^{6+} ions are 497.51 and 469.48 mg/g respectively. According to kinetic studies,

the pseudo-second-order model was used to remove both Cu^{2+} (R^2 = 0.9996) and Cr^{6+} (R^2 = 0.9986) ions from wastewater. In conclusion, it was determined that CS-NPs/AL/HAP composite material would be a better biosorbent for heavy metal ion removal.

Keywords: CS-NPs/AL/HAP composite, Batch adsorption studies, removal of Cu^{2+} and Cr^{6+} ions, Freundlich isotherm model, adsorption kinetics.

Introduction

As the demand for clean water rises and water supplies are depleted, there is less safe drinking water available for human consumption and use today. Water pollution has become a severe worldwide environmental problem in the last ten years due to fast industrialization and urbanisation, and in this context, the metal ions present in wastewater have been a growing source of concern [1–4]. The beneficial uses of water are reduced when it is contaminated with too many heavy metals because of their toxicity and other negative impacts they have on living organisms [5,6]. Lead, nickel, copper, mercury, chromium, cadmium, and arsenic are some of the most prevalent heavy metals, and they are released during dental procedures, textile production, tanning, electroplating, and the paper and pulp sector [1,3,7,8].

More importantly, because of non-biodegradability, bioaccumulation, and biomagnification of heavy metals in the food chain, they can easily access and go into our lives and pose serious health risks [9–11]. They cause a range of diseases in humans, including cancer, Alzheimer's, Parkinson's, bone mineralization, effects on DNA and RNA, and problems with the reproductive system [12]. Children with mental disorders are more likely to have heavy metal toxicity than adults with dementia, major organ dysfunction, depression, eyesight problems, and emotional disturbances [12,13]. Although many organs, including both plants and humans, require extremely little amounts of heavy

metals for normal activities, when their concentrations crosses limit, they become hazardous [1,11].

The difficulty of removal is further increased by the presence of metal ions in various forms, such as Cr primarily in their anionic forms ($HCrO_4^-$), and Cu in their cationic forms (Cu^{2+}) [2,14,15]. Chromium is the seventh most prevalent element on earth [16–18], and is spread to both groundwater and surface water [19,20]. This is due to its wide industrial applications. Chromate ions (CrO_4^{2-}), which frequently go across cellular and nuclear membranes via anion transporter pathways (such as for sulphate), pass through them fast while the trivalent species take longer to do so, according to research on the carcinogenicity of Cr(VI) [21]. An vital trace element for human and animal health, Cr(III) is required for the metabolism of lipids and sugars [22]; nevertheless, plants do not need it [23]. For instance, when the amount of copper ions in the body is too high, it can lead to Parkinson's disease [24], Alzheimer's disease [25], and other diseases, as well as disrupt mitochondrial function and integrity [26]. Heavy metal contaminants have been removed from aqueous solutions using a variety of techniques, including adsorption, photocatalysis, membrane technology, ion exchange, coagulation, etc [27–30].

As a result, creating effective methods for the sorption of heavy metals is crucial for protecting both human health and the environment. The most effective, feasible, and affordable process to eliminate heavy metals from industrial effluents is through the adsorption process. Different polymers and biopolymers are used as adsorbents has drawn a lot of attention recently [31,32]. Chitosan and its derivatives are the highly efficient biosorbents for the elimination of heavy metal contaminants from the aquatic environment. The amino polysaccharide chitosan is produced by deacetylating chitin (poly-N-acetyl-D-glucosamine), the second-most prevalent biopolymer in nature after

cellulose [33–35]. Biodegradability, biocompatibility, hydrophilicity, nontoxicity, antibacterial activity, low immunogenicity, affordability, and accessibility are just a few of the amazing qualities of chitosan [35–37].

Nano-sized adsorbents perform better than conventional micro-sized supports used in separation processes because of their high specific surface area, small size, and quantum size effect, which may cause them to have higher metal ion capacity [38,39]. Hence in the present work, chitosan was converted into chitosan nanoparticles to perform better adsorption process. Also to improve the efficiency, chitosan nanoparticles was mixed with sodium alginate and novel hydroxyapatite (HAp) extracted from *Scomberomorus guttatus*. Alginates are low-cost valuable linear block copolymers of two uronic acid residues, such as β-D-mannuronic and β-l-guluronic acid, and are joined by β-1,4-glycosidic linkages. This biopolymer has been utilised extensively in wastewater treatment because of its stability, high water permeability, biodegradability, and nontoxic nature for the adsorption of contaminants, especially heavy metal cations. [40–43].

According to Ahmad and Mirza, the performance of nanosorbents and their biosorption capabilities can be improved by alginate and its nanocomposite could be recycled five times successfully [44]. As a potential alternative adsorbent for the adsorptive treatment of dye- and heavy metal-contaminated wastewater, hydroxyapatite (HAp) and its derivatives have come to light [45–47]. This is due to their unique characteristics and structure such as surface, the acidity and basicity, the surface charge, the hydrophilicity, and the porosity of HAp's surface, which give them the capacity to exchange ions, have low water solubility, be thermally stable, and have a high adsorption affinity for a variety of contaminants [47]. It has been discovered that the HAp surface has

2.6 nm^2 of P-OH groups that serve as sorption sites [48]. For both industrial processes and environmental processes, HAp's sorption capabilities are crucial [49].

Since there are many reports on chitosan nanoparticles composites in heavy metal removal applications, in this study the natural hydroxyapatite extracted from vanjaram fish bone was used to prepare a novel ternary biocomposite o-vanillin crosslinked chitosan nanoparticles/alginate/hydroxyapatite (extracted from vanjaram fish bone) biocomposite to removal of heavy metals copper and chromium. The prepared material was characterized using FTIR, XRD and SEM. The batch mode of adsorption was performed by varying the affecting parameters such as pH, adsorbent dose, contact time and initial metal ion concentration. The experimental data was validated using the theoretical models such as Langmuir isotherm, Freundlich isotherm, pseudo-first order kinetics and pseudo-second order kinetics.

Materials and methods

Materials

Indian Seafoods in Cochin, Kerala, is where chitosan was purchased. Nice Chemicals Private Ltd. provided the sodium alginate. Thermo Fisher Scientific private Ltd. India supplied the sodium alginate and carboxymethyl cellulose. The Indian company SD-fine-chemicals Limited supplied the crosslinking agent, o-vanillin. The solutions were made using only analytical reagent grade reagents. Vanjaram fish was used as a source of hydroxyapatite (HAp) (*Scomberomorus guttatus*). The fish bone was well ground and roasted for an hour in the oven before being fried for an hour to produce a black mixture of fish bone. Once more, it spent two days being heated to 800 °C for five hours in the muffle furnace. It was acquired and put to use in its pure, white powder form.

Preparation of chitosan nanoparticles (CS-NPs)

200 mL of 2% acetic acid solution was used to dissolve 1 g of chitosan while it was being mechanically stirred. The chitosan solution received 0.8 g of sodium tripolyphosphate (TPP), dissolved in 107 ml of double-distilled water, dropwise, and was vigorously stirred for two hours [50]. The suspension was allowed to settle before the supertanant was decanted. The generated chitosan nanoparticles were washed in water until a pH of 6 was obtained.

Preparation of chitosan nanoparticles (CS-NPs)/Alginate (AL)/Hydroxyapatite (HAP) + o – vanillin crosslinked biocomposite

In order to create a homogeneous solution, 0.5 g of hydroxyapatite was added while stirring steadily after 1 g of sodium alginate and 1 g of chitosan nanoparticles were combined. The composite was then crosslinked by adding approximately 4 g of o-vanillin dissolved in 20 mL of ethanol and vigorously stirring for an hour with a mechanical stirrer (8000 rpm). Finally, the composite was allowed to dry.

Batch adsorption studies

To create a 100 ppm stock solution, 0.283 g of potassium dichromate and 0.3929 g of copper sulphate are precisely weighed and separately dissolved in one litre of double-distilled water. After that, batch mode was implemented using this solution. Cr(VI) and Cu(II) ions were adsorbed onto the o-vanillin crosslinked CS-NPs/AL/HAP adsorbent using a batch adsorption technique. The variables included temperature, pH, contact time, adsorbent dosage, and initial metal ion concentration. In the separate conical flask, 50 mL of Cu(II) ion solution and 50 mL of Cr(VI) ion solution were taken. This was mixed with 0.1 g of adsorbent each and shaken at 200 rpm for an hour. The reaction mixture was filtered using Whatmann filter paper after shaking for an hour, and the pH was then adjusted by adding 2 N HCl and 2 N NaOH. The filtered solution was then subjected to an AAS analysis to measure

the concentration of Cu(II) and Cr(VI) ions. The same methodology has been used to study the effects of initial metal concentration, adsorbent dosage, pH, contact time, and temperature. The following equation was used to calculate the removal percentage (%) and adsorption capacity (mg/g) after the adsorption process [51].

$$Removal\ (\%) = \frac{C_0 - C_e}{C_0}\ x\ 100$$

$$Adsorption\ capacity\ (q_e) = \frac{C_0 - C_e}{M}\ x\ V$$

where C_o and C_e are the initial and final metal ion concentrations, V is the volume of the solution in litre and M is the weight of dry adsorbent in gram [51].

Instrumental analysis

FTIR measurements were performed using a Perkin Elmer 200 FT-IR spectrophotometer and pellets of potassium bromide. The wavenumber range for the FTIR spectra was 4000 cm^{-1} to 450 cm^{-1}. The crystallinity of the produced samples was evaluated using an X-ray powder diffractometer (XRD - SHIMADZU XD - D1) and a Ni-filtered Cu Kα X-ray radiation source. Scanning electron microscope surface imaging was investigated using the JEOL JSM-6390LV at a voltage of 20 kV.

Results and Discussion

FTIR

The FTIR spectrum of CS-NPs and CS-NPs/AL/HAP crosslinked with o-vanillin was given in figure 1a and 1b. O-H and N-H, the primary functional groups of CS-NPs, displayed an absorption band at 3446 cm^{-1}. During the composite's formation (o-vanillin crosslinked CS-NPs/AL/CMC biocomposite), it was pushed to the lower wavenumber region of 3313 cm^{-1}, showing a significant interaction between the polymers. The two bands (OH and NH) in the chitosan samples overlap despite being distinct and spaced

apart due to hydrogen bonding. As a result, both the O-H and N-H groups displayed a broadband in the same region [52].

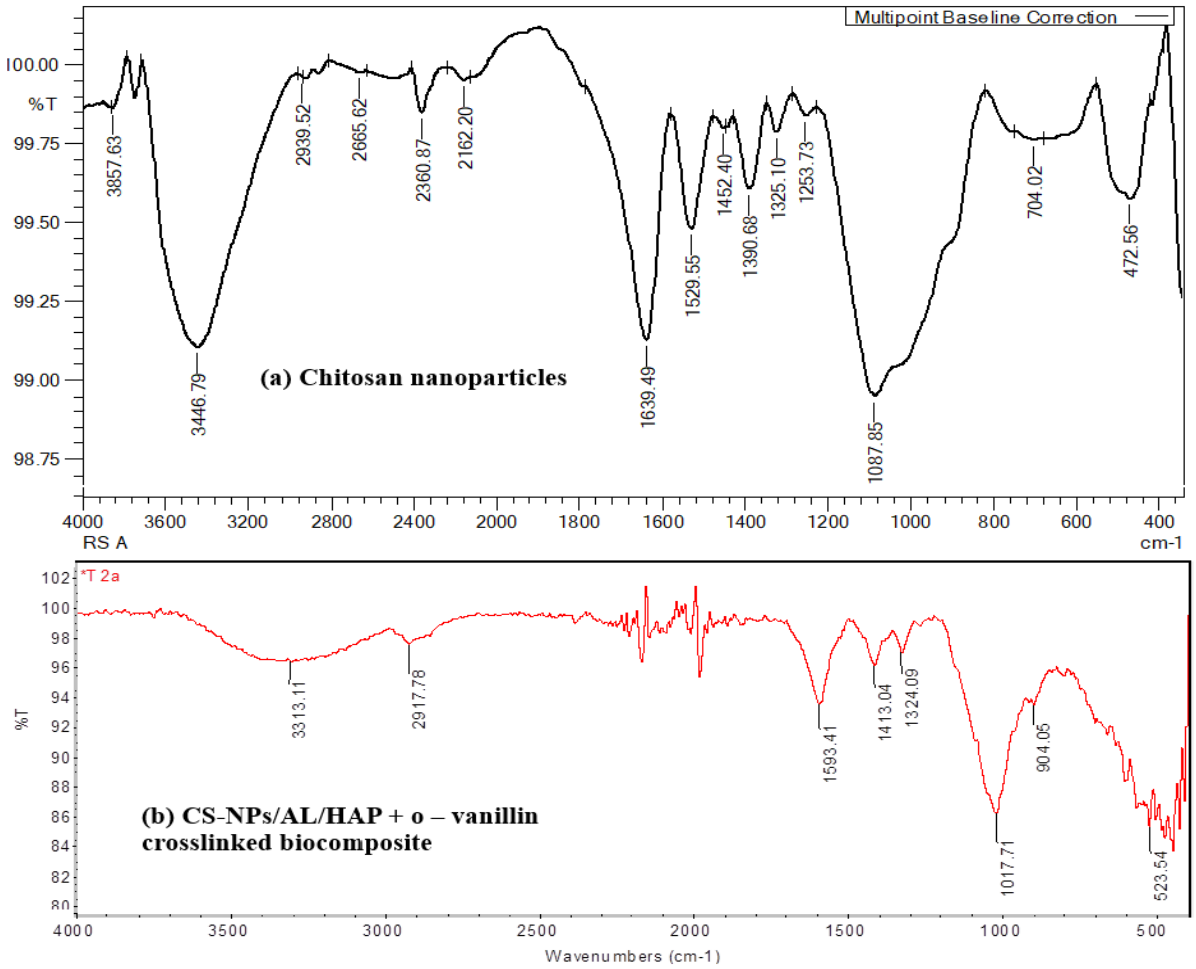

Figure 1: FTIR spectrum of (a) chitosan nanoparticles and (b) chitosan nanoparticles (CS-NPs)/ Alginate (AL)/ Hydroxyapatite (HAP) + o – vanillin crosslinked biocomposite

The existence of C-H stretching in CS-NPs and the CS-NPs/AL/HAP + o-vanillin composite is shown by the bands seen at 2939 and 2917 cm^{-1}, respectively. For chitosan nanoparticles, the band for C=O stretching, N-H bending, C-H bending, C-O stretching, and P-O stretching modes emerged at 1639, 1529, 1390, 1325, and 1087 cm^{-1}; for CS-NPs/AL/HAP + o-vanillin composite, it appeared at 1593, 1413, 1324, and 1107 cm^{-1}.

Additionally, the band at 1639 cm^{-1} in chitosan nanoparticles vanished in the composite, indicating the development of hydrogen bonds between polymers, when compared to the FTIR spectra of chitosan nanoparticles and the absorption bands of CS-NPs/AL/HAP + o-vanillin composite. The main functional groups, such as OH, NH, COO-, C=O, and P-OH, showed a significantly shifted band in the prepared composite, indicating that these groups were involved in the successful formation of the CS-NPs/AL/HAP + o-vanillin composite via covalent bonding, electrostatic binding, hydrogen bonding, and van der Waals forces (Sugashini et al., 2022).

XRD

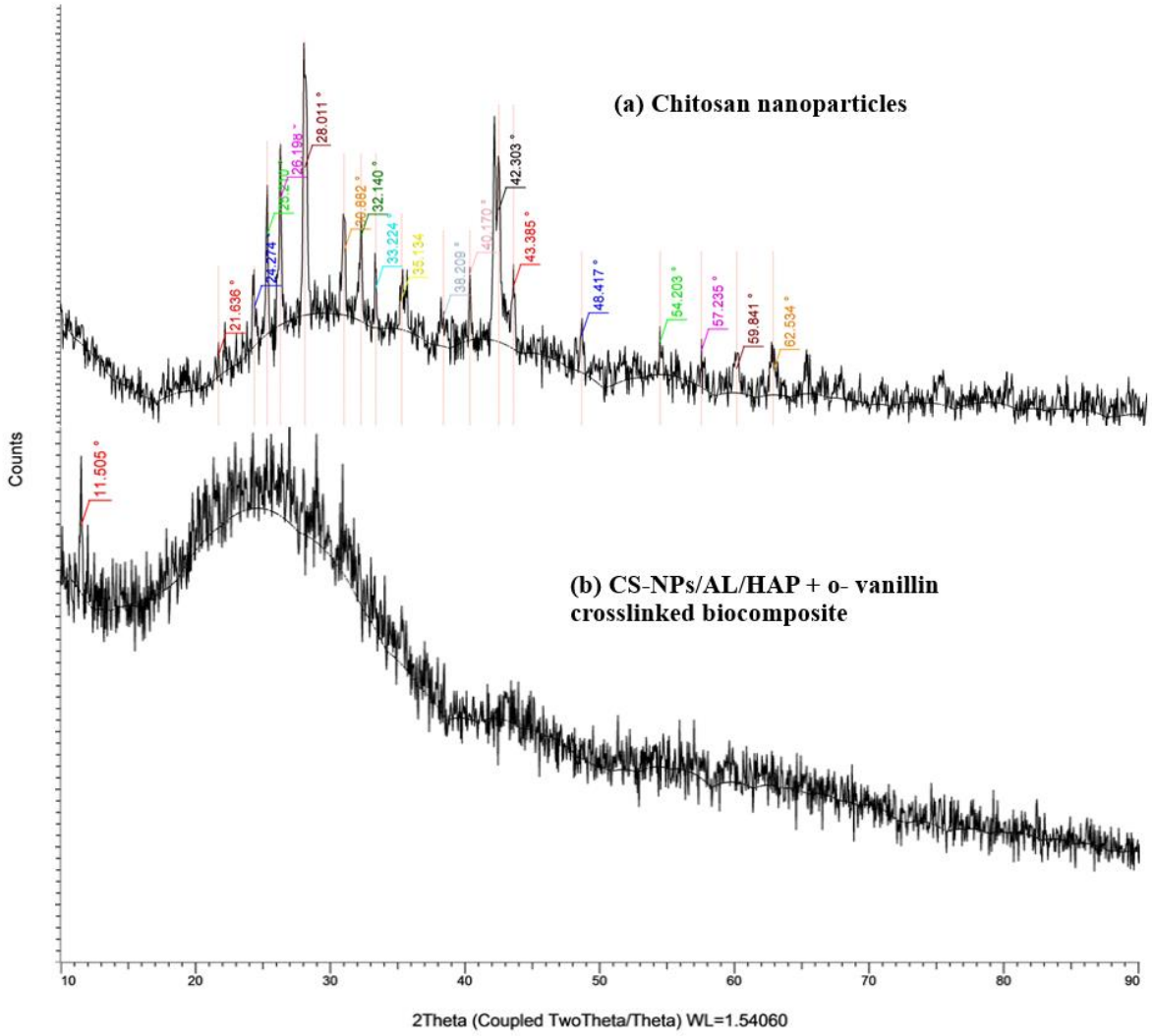

Figure 2: XRD pattern of (a) chitosan nanoparticles and (b) chitosan nanoparticles (CS-NPs)/ Alginate (AL)/ Hydroxyapatite (HAP) + o – vanillin crosslinked biocomposite

As can be seen, the main broad diffraction peaks for CS-NPs and its composite were at 2θ = 30° and 25°, respectively. The broad peak indicated that CS-NPs and its composite had low crystallinity. Additionally, the dense network structure and intermolecular contact generated between the primary functional groups of the additional polymers was the cause of the observed breakdown in the structure of the prepared composite. Additionally, during the blending of AL, HAP, and o-vanillin with CS-NPs, a shift in the peak of the CS-NPs/AL/HAP + o-vanillin composite to the lower region was observed. The prepared composite's observed peak shift demonstrated the intermolecular interactions between the polymers.

Bath adsorption studies

Effect of pH

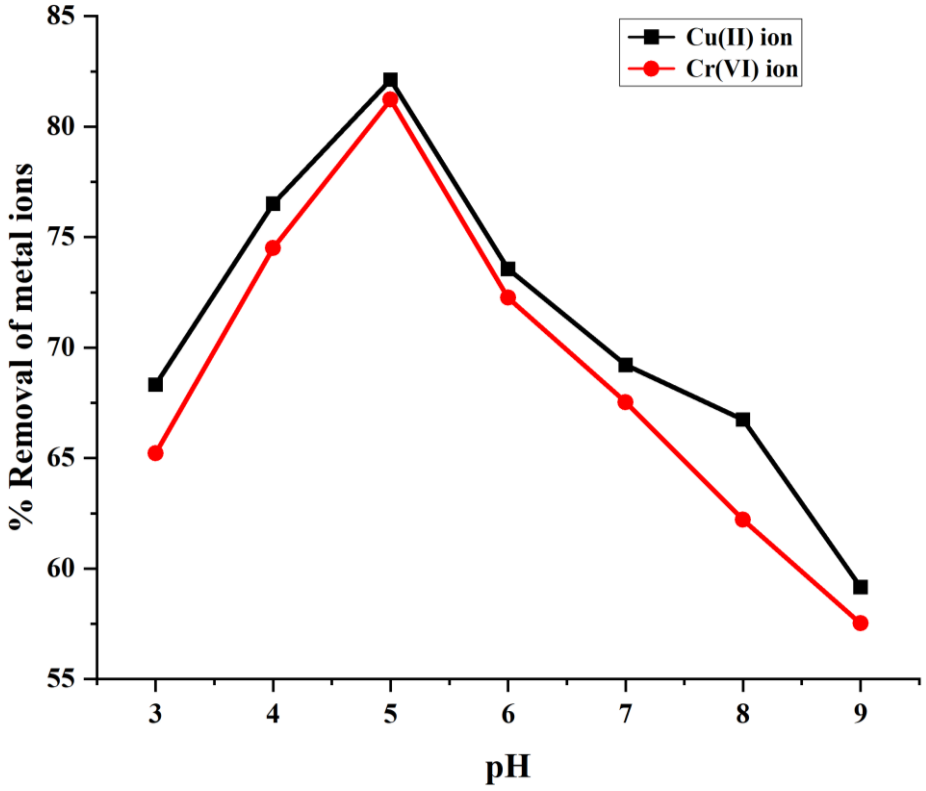

Figure 3: Effect of metal ion pH

Heavy metals copper and chromium removal by o-vanillin crosslinked CS-NPs/AL/HAP biocomposite from aqueous solution was thought to be significantly influenced by pH, because pH affects the surface charge of the composite nanomaterial as well as the speciation of the contaminants. Thus, in the study the metal ion pH was varied from 3 to 9 (adsorbent dose 0.1 g; contact time 60 min; initial concentration 100 ppm) in order to investigate its effect during adsorption (Figure 3). The result indicates that, the pH of the adsorption medium directly affects the form of Cr in aqueous solutions. Cr(VI) exists as H_2CrO_4 at pH 1, $Cr_2O_7^{2-}$ and $HCrO_4^-$ at pHs between 2 and 6, and CrO_4^{2-} is the dominant form at pHs greater than 6. The electrostatic interaction between hereto groups of chitosan and the neutral H_2CrO_4 molecules is thereby reduced as a result of Cr(VI) being present in a neutral state (H_2CrO_4) at pH 1 [54,55].

At pH 2, NH_2 groups of undergo protonation, increasing the positive charges on the adsorbent surface. As a result, there was an improvement in the adsorption process due to the stronger electrostatic attraction forces between the positively charged NH_3^+ groups and the negatively charged Cr(VI) ions. On the other hand, the protonation of NH_2 groups and the positive charges on the surface of chitosan significantly diminish above pH 2. Therefore, there is a reduction in the columbic interaction between chitosan and Cr(VI) [56,57].

At various pH values, the copper ion in aqueous solution would exist as Cu^{2+}, $Cu_2(OH)_2^{2+}$, $Cu(OH)^+$, $Cu_2(OH)_3^+$, $Cu_3(OH)_4^{2+}$, and $Cu(OH)_2$ [58]. Then, $Cu(OH)_2$ has a Ksp (solubility product) value of $5.6x10^{-20}$, indicating that there is a chance that it will precipitate at pH levels higher than 6, which also indicated that Cu(II) will leave the solution through precipitation [58].

Effect of contact time

The effect of contact time is the important parameter to scale up the adsorption process to industrial level. To evaluate the effect of contact time the experiment was carried out by varying the time from 60 to 300 min by keeping other parameters adsorbent dose (0.1 g), pH 5, initial concentration (100 ppm) and temperature as constant. The results were given in figure 4. From the results it was revealed that due to the speedy transfer of metal contaminants from the solution to the active sites of the biosorbent, the adsorption rates increases rapidly initially with increasing time [38,59]. However, when some of the readily accessible active sites have been occupied, metal requires time to identify more active sites for binding. After sometimes the adsorption rates dropped and did not alter significantly even the period was extended, due to the saturation of active

adsorbent site. Thus, it was determined that for optimal outcomes, metal and composite should be in contact for 300 min for both copper and chromium.

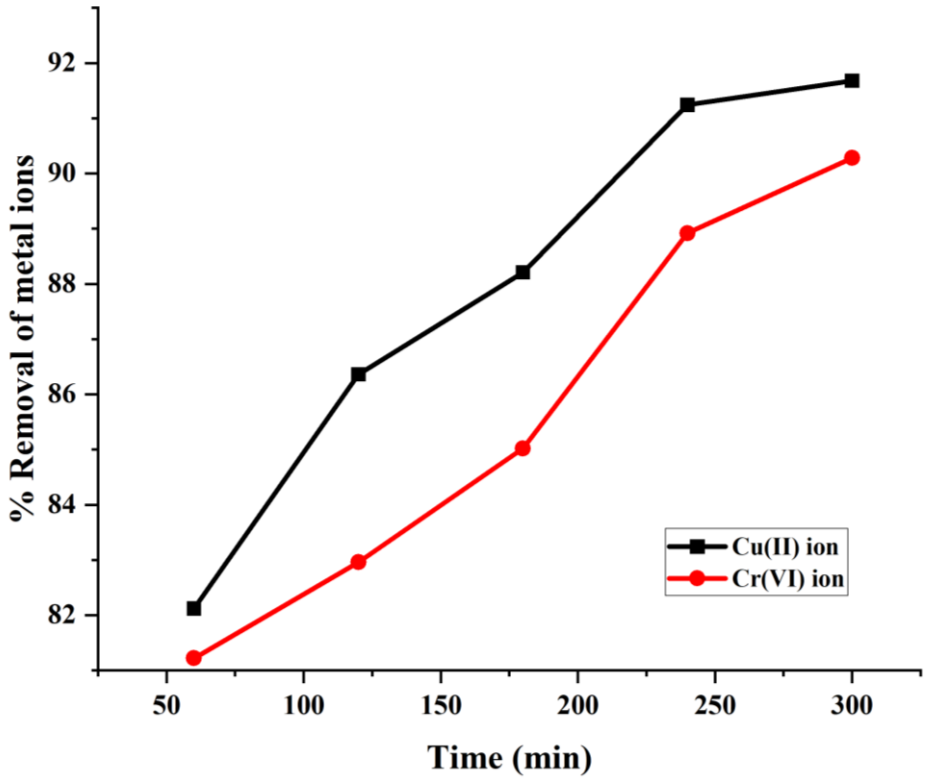

Figure 4: Effect of contact time on the removal of Cu(II) ion and Cr(VI) ion using CS-NPs/AL/HAp biocomposite

Adsorbent dose

According to a study on the influence of adsorbent dosage on metal adsorption, the amount of CS-NPs/AL/HAp biocomposite had an impact on the amount of metals that were adsorbed (Figure 5). As shown in Figure 5, the minimum percentage removal for copper was 82.12% for the dose of 0.1 g and the maximum percentage removal was 92.64% foe 0.5 g of adsorbent dose. For chromium it was ranged from 81.22% for the dose of 1 g to 90.23% for the dose of 0.5 g.

The fact that additional surface area is available for adsorption to occur may be the cause of the increase in adsorption with the increase of adsorbent dose. By increasing the

sorbent, there are more adsorption sites accessible, that improves the removal efficiency [60]. In conclusion, the removal efficiency of CS-NPs/AL/HAp biocomposite increased with increasing adsorbent dose and achieved equilibrium at around 0.5 g.

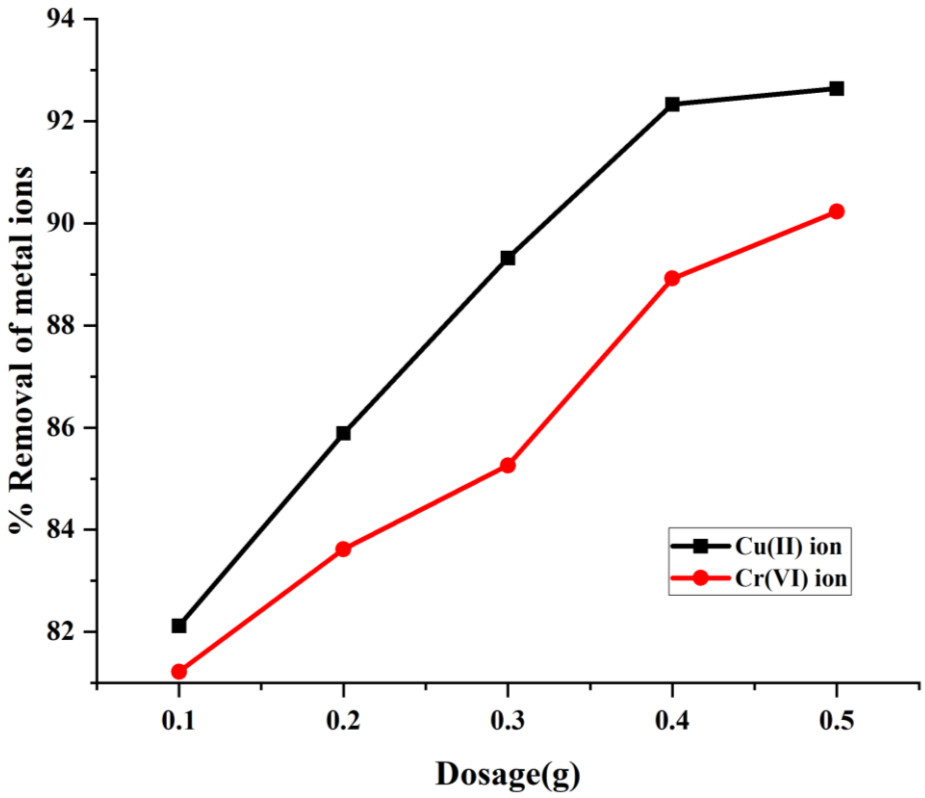

Figure 5: Effect of adsorbent dose on the removal of Cu(II) ion and Cr(VI) ion using CS-NPs/AL/HAp biocomposite

Effect of initial concentration

CS-NPs/AL/HAp biocomposite was used to sorb Cu^{2+} and Cr^{6+} ions at various initial metal ion concentrations ranging from 50 to 500 mg/L, at pH 5, at 120 rpm, and for 60 minutes of contact time. The removal of Cu(II) and Cr(VI) ions by sorbent took place in a quick kinetic process (Figure 6). As compared to the original concentration, the aqueous metal ion concentration decreased. A higher initial metal concentration led to an increase in the metal ion's uptake, which eventually tended to reach saturation.

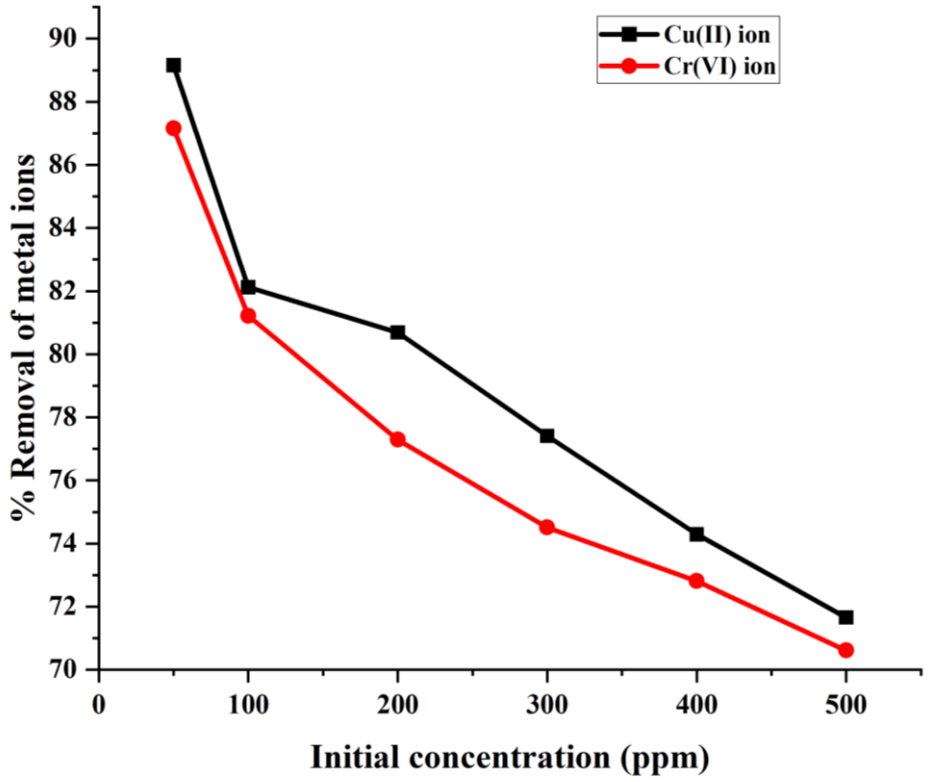

Figure 6: Effect of initial metal ion concentration on the removal of Cu(II) ion and Cr(VI) ion using CS-NPs/AL/HAp biocomposite

Sorption Efficiency

The ratio of the metal ion adsorbed to the amount in the liquid phase is known as an adsorbent's distribution coefficient (K_d) [61]. Low sorption efficiency is indicated by distribution coefficient values that are less than 1.0. The following equation can be used to compute the K_d.

$$K_d = \frac{q_e}{C_e}$$

where

q_e = amount of metal ions adsorbed.

C_e = amount of metal ion in liquid phase.

Table 1: Distribution co-efficient of Cu(II) and Cr(VI) ions

Initial concentration of metal ions (ppm)	**Cu(II)**			**Cr(VI)**		
	C_{ads}	C_{eq}	K_d	C_{ads}	C_{eq}	K_d
500	358.3	141.7	2.5286	353.05	146.95	2.4025
400	297.16	102.84	2.8895	291.24	108.76	2.6778
300	232.23	67.77	3.4267	223.53	76.47	2.9231
200	161.38	38.62	4.1787	154.58	45.42	3.4033
100	82.12	17.88	4.5928	81.22	18.78	4.3248
50	44.58	5.42	8.2251	43.58	6.42	6.7882

Cr ion distribution coefficient spans from 2.4025 to 6.7882, while Cu ion vary from 2.5286 to 8.2251. As shown in Table 1, the values of the metal ion distribution coefficient between the CS-NPs/AL/HAp biocomposite and the aqueous phase in this investigation depend on the metal ion concentrations at the beginning of the experiment and are higher than 1.0. The CS-NPs/AL/HAp biocomposite showed high efficiency for the treatment of wastewater containing Cu^{2+} and Cr^{6+} ions, according to the estimated values of the distribution coefficient (K_d) in Table 1.

Adsorption isotherm

The required adsorption equilibrium is necessary for the analysis and design of the adsorption system, which is the most crucial step in comprehending an adsorption process. Adsorption equilibria offer key physicochemical information for determining if the adsorption mechanism may be used as a standalone unit operation [62]. The plot of C_{eq}/C_{ads} vs C_{eq} and log C_{ads} vs log C_{eq} yielded a straight line (Figure 7 and 8) gives the Langmuir adsorption isotherm and Freundlich adsorption isotherm and the calculated parameters are given in the table 1.

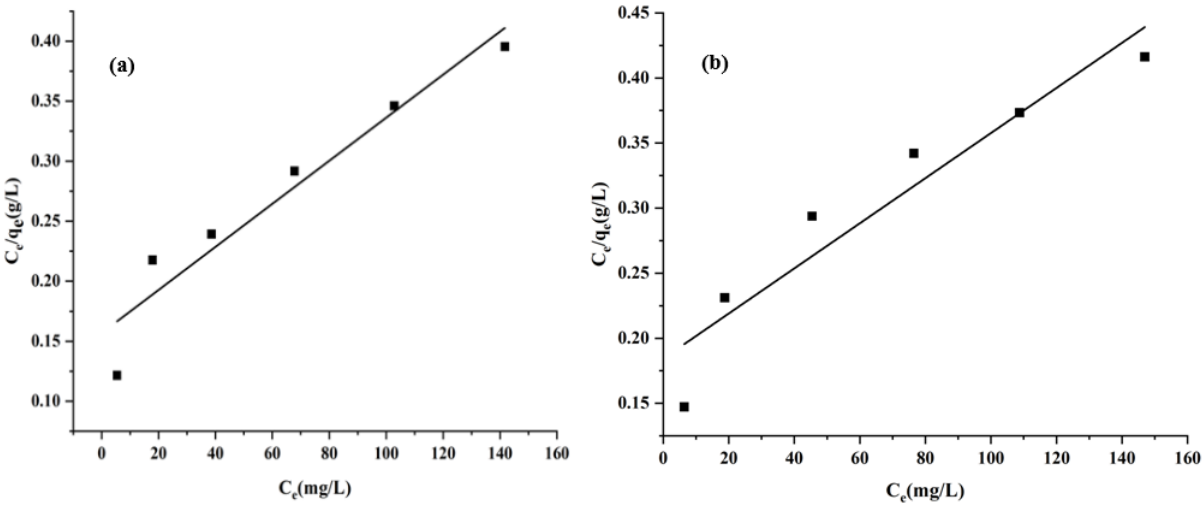

Figure 7: Langmuir isotherm models for the removal of (a) Copper and (b) Chromium

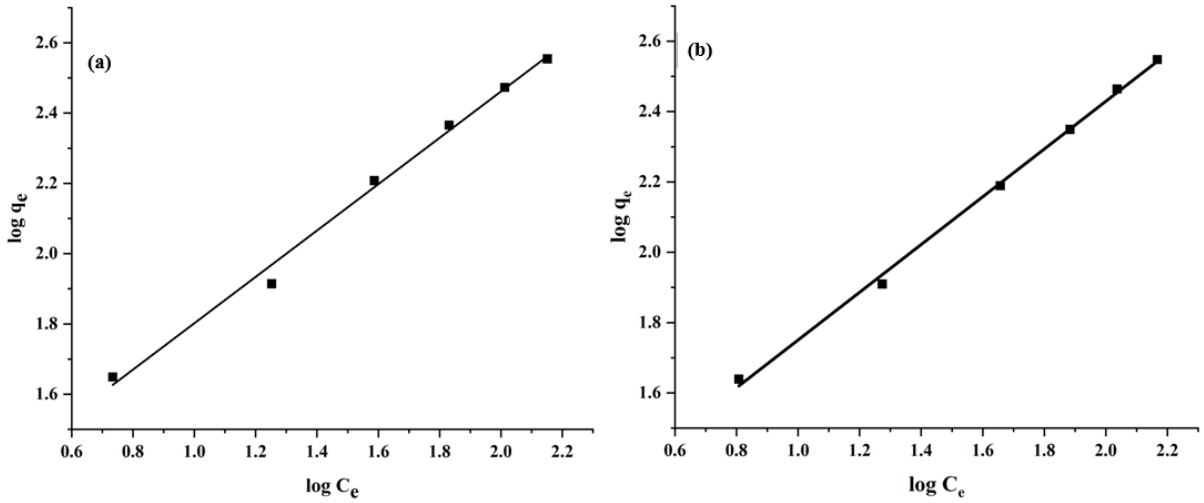

Figure 8: Freundlich isotherm models for the removal of (a) Copper and (b) Chromium

Table 2: Langmuir and Freundlich isotherm constants for the adsorption of Cu^{2+} ion using CS-NPs/AL/HAP + o-vanillin biocomposite

Metal ion	Langmuir isotherm $\frac{C_{eq}}{C_{ads}} = \frac{b\,C_{eq}}{K_L} + \frac{1}{K_L}$				Freundlich isotherm $\log C_{ads} = \log K_F + \frac{1}{n}\log C_{eq}$		
	K_L (dm^3/g)	**b (dm^3/mg)**	**C_{max}**	**R^2**	**K_F**	**n**	**R^2**
Cu(II)	6.3776	0.0128	497.51	0.9273	13.8739	1.5161	0.9933
Cr(VI)	5.4259	0.0116	469.48	0.9051	11.7978	1.4741	0.9979

A monolayer of adsorbate had formed on the surface of the adsorbent, according to the Langmuir plot. Compared to Cr(VI), Cu(II) had a higher C_{max} value. For CS-NPs/AL/HAp ternary biocomposite, the C_{max} values were 497.51 mg of Cu(II), and 469.48 mg of Cr(VI). R^2 value indicated a linear or correlating relationship. In the instance of the Freundlich isotherm model, the relationship got more linear with the value that was closest to 1. As a result, it was discovered that during concentration studies, the adsorption of Cu(II), and Cr(VI) ions onto CS-NPs/AL/HAp ternary biocomposite well correlated with the Freundlich isotherm model than Langmuir isotherm.

Table 2 displays the values of n and K_F, which were determined from the slopes and intercepts of the Freundlich plots (Figure 8), respectively. n values between 1 and 10 demonstrated advantageous adsorption, according to Kadirvelu and Namasivayam, (2000). The values of n and K_F also affect the isotherm's curvature and steepness, according to Akgerman and Zardkoohi, (1996). The Freundlich equation, despite not having any theoretical foundation, provided adequate information about the adsorption data over a specific concentration range. A multi-layer adsorption was evident from the lack of a plateau in the adsorption isotherm [65].

Thus, the study concludes that the adsorption procedure used in the current investigation is physisorption with multilayer adsorption. Based on the isotherm models, the outcome showed that the prepared o-vanillin crosslinked CS-NPs/AL/HAp ternary biocomposite followed heterogeneous (or) multilayer adsorption.

Adsorption kinetics

Using pseudo-first and pseudo-second order equations, the mechanism of adsorption was examined, and rate constants for the adsorption of copper, and chromium ions were

found. Cu(II), and Cr(VI) uptake by o-vanillin crosslinked CS-NPs/AL/HAp ternary biocomposite sorption data were fitted using Lagergren pseudo-first-order (Figure 9) and pseudo-second-order models (Figure 10). The plot of t vs log ($q_e - q_t$) and t vs t/q_t gives the value of k_1, k_2 and q_e from its slope and intercept respectively [60].

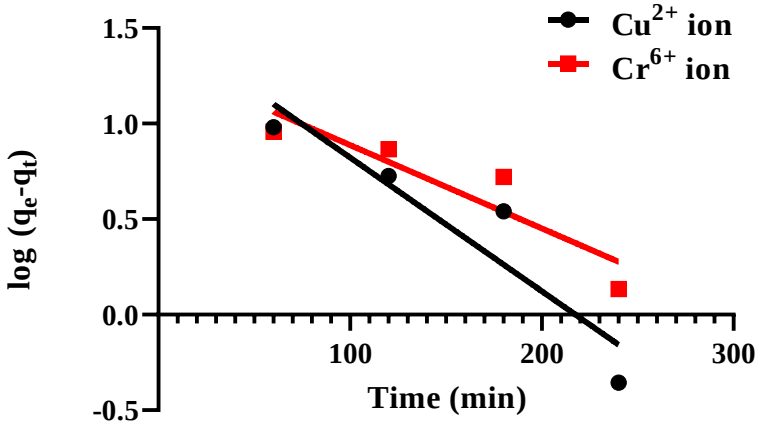

Figure 9: Pseudo-first order kinetics

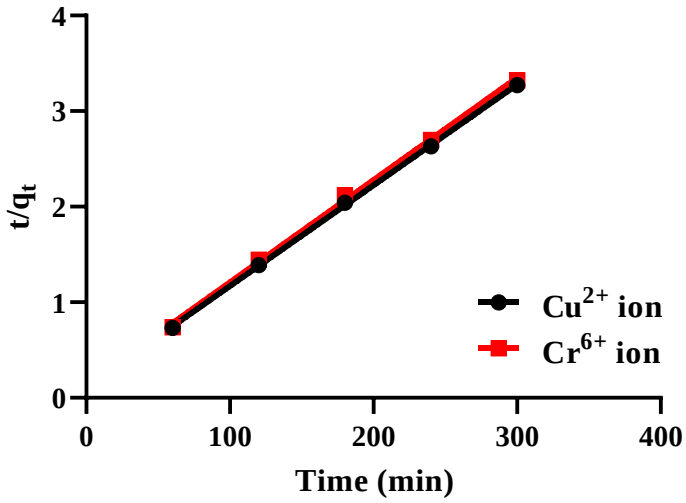

Figure 10: Pseudo-second order kinetics

Table 3: Adsorption kinetic studies for the adsorption of Cu^{2+} ion using CS-NPs/AL/HAP + o-vanillin biocomposite

Metal ion	Pseudo-first order $log\ (q_e - q_t) = \log q_e - \frac{k_1 t}{2.303}$			Pseudo-second order $\frac{t}{q_t} = \frac{1}{k_2 q_e^2} + \frac{1}{q_e t}$		
	q_e (mg/g)	**k_1**	**R^2**	**q_e (mg/g)**	**k_2**	**R^2**
Cu(II)	33.266	0.01611	0.8683	94.8766	0.000963	0.9996
Cr(VI)	21.0378	0.010041	0.8318	96.8992	0.00083	0.9986

A comparison of two kinetic models revealed that the pseudo-second-order kinetic model's correlation coefficient (R^2) was higher than that of the pseudo-first-order model (Table 3). In contrast to the pseudo-first-order model, the obtained Cu(II), and Cr(VI) kinetic data clearly followed the pseudo-second-order kinetic model.

In general, the pseudo first-order kinetic model only applies to the early stages of the adsorption process and does not adequately describe the entire process [66–68], whereas the pseudo second-order model adequately describes the experimental data. The pseudo first-order model's less successful fitting findings demonstrated that more than one mechanism was at work throughout the adsorption process and that biosorption was not limited to one site per ion [69]. Instead of existing as dissociated ions in solution, copper, and chromium are most commonly found as hydrated complexes. Thus, the pseudo second-order kinetic model's applications can be explained by the fact that biosorption is a two-step process that involves the dissociation of hydrated complexes and the interaction of metals with active sites in the biosorbents [70].

Conclusion

In this study, novel CS-NPs/AL/HAP + o-vanillin biocomposite was developed as the promising adsorbent for the removal of copper and chromium from the aqueous solution. The FTIR and XRD analysis proves the formation of biosorbent through change in band position and broad peak. Batch adsorption studies revealed that the prepared ternary biocomposite removes copper ion more effectively than chromium ion from the aqueous solution and the sorption capacity was strongly depends on the adsorption parameters. On fitting the experimental data in theoretical isotherm model such as Langmuir and Freundlich model, the data fitted well with the Freundlich adsorption isotherm, indicating the multilayer adsorption. Also the kinetics studied proves that the experimental batch adsorption data correlated more with pseudo-second order kinetics than pseudo-first order kinetics model.

References

[1] A.U. Rehman, S. Nazir, R. Irshad, K. Tahir, K. ur Rehman, R.U. Islam, Z. Wahab, Toxicity of heavy metals in plants and animals and their uptake by magnetic iron oxide nanoparticles, J. Mol. Liq. 321 (2021) 114455. https://doi.org/https://doi.org/10.1016/j.molliq.2020.114455.

[2] S. Mao, M. Gao, Functional organoclays for removal of heavy metal ions from water: A review, J. Mol. Liq. 334 (2021) 116143. https://doi.org/https://doi.org/10.1016/j.molliq.2021.116143.

[3] H. Karimi-Maleh, A. Ayati, S. Ghanbari, Y. Orooji, B. Tanhaei, F. Karimi, M. Alizadeh, J. Rouhi, L. Fu, M. Sillanpää, Recent advances in removal techniques of Cr(VI) toxic ion from aqueous solution: A comprehensive review, J. Mol. Liq. 329 (2021) 115062. https://doi.org/https://doi.org/10.1016/j.molliq.2020.115062.

[4] F. Karimi, A. Ayati, B. Tanhaei, A.L. Sanati, S. Afshar, A. Kardan, Z. Dabirifar, C. Karaman, Removal of metal ions using a new magnetic chitosan nano-bio-adsorbent; A powerful approach in water treatment, Environ. Res. 203 (2022) 111753. https://doi.org/https://doi.org/10.1016/j.envres.2021.111753.

[5] W.C. Chang, G.S. Hsu, S.M. Chiang, M.C. Su, Heavy metal removal from aqueous solution by wasted biomass from a combined AS-biofilm process, Bioresour. Technol. 97 (2006) 1503–1508. https://doi.org/https://doi.org/10.1016/j.biortech.2005.06.011.

[6] L. Altaş, Inhibitory effect of heavy metals on methane-producing anaerobic granular sludge, J. Hazard. Mater. 162 (2009) 1551–1556. https://doi.org/https://doi.org/10.1016/j.jhazmat.2008.06.048.

[7] B. Volesky, Detoxification of Metal-Bearing Effluents: Biosorption for the Next Century, Hydrometallurgy. 59 (2001) 203–216. https://doi.org/10.1016/S0304-386X(00)00160-2.

[8] H. Zhang, Y. Zhao, Z. Wang, Y. Liu, Distribution characteristics, bioaccumulation and trophic transfer of heavy metals in the food web of grassland ecosystems, Chemosphere. 278 (2021) 130407. https://doi.org/https://doi.org/10.1016/j.chemosphere.2021.130407.

[9] A.S. Abdel-Baki, M.A. Dkhil, S. Al-Quraishy, Bioaccumulation of some heavy metals in tilapia fish relevant to their concentration in water and sediment of Wadi Hanifah, Saudi Arabia, African J. Biotechnol. (2011). https://doi.org/10.5897/AJB10.1772.

[10] M. Jaishankar, B.B. Mathew, M.S. Shah, K.M. T.P., S.G. K.R., Biosorption of Few Heavy Metal Ions Using Agricultural Wastes, J. Environ. Pollut. Hum. Heal. 2 (2014) 1–6. https://doi.org/10.12691/jephh-2-1-1.

[11] P.C. Nagajyoti, K.D. Lee, T.V.M. Sreekanth, Heavy metals, occurrence and toxicity

for plants: a review, Environ. Chem. Lett. 8 (2010) 199–216. https://doi.org/10.1007/s10311-010-0297-8.

[12] A.T. Jan, M. Azam, K. Siddiqui, A. Ali, I. Choi, Q.M.R. Haq, Heavy Metals and Human Health: Mechanistic Insight into Toxicity and Counter Defense System of Antioxidants, Int. J. Mol. Sci. 16 (2015) 29592–29630. https://doi.org/10.3390/ijms161226183.

[13] A.T. Jan, A. Ali, Q. Haq, Glutathione as an antioxidant in inorganic mercury induced nephrotoxicity., J. Postgrad. Med. 57 (2011) 72–77. https://doi.org/10.4103/0022-3859.74298.

[14] T. Şahan, F. Erol, Ş. Yılmaz, Mercury(II) adsorption by a novel adsorbent mercapto-modified bentonite using ICP-OES and use of response surface methodology for optimization, Microchem. J. 138 (2018) 360–368. https://doi.org/10.1016/j.microc.2018.01.028.

[15] C. Xiong, S. Wang, P. Hu, L. Huang, C. Xue, Z. Yang, X. Zhou, Y. Wang, H. Ji, Efficient Selective Removal of Pb(II) by Using 6-Aminothiouracil-Modified Zr-Based Organic Frameworks: From Experiments to Mechanisms, ACS Appl. Mater. Interfaces. 12 (2020) 7162–7178. https://doi.org/10.1021/acsami.9b19516.

[16] B. Saha, C. Orvig, Biosorbents for hexavalent chromium elimination from industrial and municipal effluents, Coord. Chem. Rev. 254 (2010) 2959–2972.

[17] P. Senthil Kumar, M. Yashwanthraj, Sequestration of toxic Cr(VI) ions from industrial wastewater using waste biomass: A review, Desalin. WATER Treat. 68 (2017) 245–266. https://doi.org/10.5004/dwt.2017.20322.

[18] P. Senthil Kumar, R. Sivaranjanee, P. Sundar Rajan, A. Saravanan, Carbon sphere: Synthesis, characterization and elimination of toxic Cr(VI) ions from aquatic system, J.

Ind. Eng. Chem. 60 (2018) 307–320. https://doi.org/https://doi.org/10.1016/j.jiec.2017.11.017.

[19] B. Zhou, D. Huang, J. Wu, Q. Zhu, H. Zhu, Horizontal and Vertical Distributions of Chromium in a Chromate Production District of South Central China, Int. J. Environ. Res. Public Health. 15 (2018). https://doi.org/10.3390/ijerph15040571.

[20] N. Ferronato, V. Torretta, Waste Mismanagement in Developing Countries: A Review of Global Issues., Int. J. Environ. Res. Public Health. 16 (2019). https://doi.org/10.3390/ijerph16061060.

[21] M. Pas, R. Milacic, K. Draslar, N. Pollak, P. Raspor, Uptake of chromium(III) and chromium(VI) compounds in the yeast cell structure., Biometals an Int. J. Role Met. Ions Biol. Biochem. Med. 17 (2004) 25–33. https://doi.org/10.1023/a:1024437802914.

[22] J. Bai, P. Xun, S. Morris, D.R. Jacobs, K. Liu, K. He, Chromium exposure and incidence of metabolic syndrome among American young adults over a 23-year follow-up: the CARDIA Trace Element Study, Sci. Rep. 5 (2015) 15606. https://doi.org/10.1038/srep15606.

[23] A.K. Shanker, C. Cervantes, H. Loza-Tavera, S. Avudainayagam, Chromium toxicity in plants, Environ. Int. 31 (2005) 739–753. https://doi.org/https://doi.org/10.1016/j.envint.2005.02.003.

[24] Y. Li, C. Yang, S. Wang, D. Yang, Y. Zhang, L. Xu, L. Ma, J. Zheng, R.B. Petersen, L. Zheng, H. Chen, K. Huang, Copper and iron ions accelerate the prion-like propagation of α-synuclein: A vicious cycle in Parkinson's disease., Int. J. Biol. Macromol. 163 (2020) 562–573. https://doi.org/10.1016/j.ijbiomac.2020.06.274.

[25] R. Squitti, C. Salustri, M. Rongioletti, M. Siotto, Commentary: The case for

abandoning therapeutic chelation of copper ions in Alzheimer's disease, Front. Neurol. 8 (2017) 10–13. https://doi.org/10.3389/fneur.2017.00503.

[26] I.L. Yurkova, J. Arnhold, G. Fitzl, D. Huster, Fragmentation of mitochondrial cardiolipin by copper ions in the Atp7b-/- mouse model of Wilson's disease., Chem. Phys. Lipids. 164 (2011) 393–400. https://doi.org/10.1016/j.chemphyslip.2011.05.006.

[27] Y. Ibrahim, V. Naddeo, F. Banat, S.W. Hasan, Preparation of novel polyvinylidene fluoride (PVDF)-Tin(IV) oxide (SnO2) ion exchange mixed matrix membranes for the removal of heavy metals from aqueous solutions, Sep. Purif. Technol. 250 (2020) 117250. https://doi.org/https://doi.org/10.1016/j.seppur.2020.117250.

[28] M. Zheng, Z. Sun, H. Han, Z. Zhang, W. Ma, C. Xu, Enhanced coagulation coupled with heavy metal capturing for heavy metals removal from coal gasification brine and a novel mathematical model, J. Water Process Eng. 40 (2021) 101954. https://doi.org/https://doi.org/10.1016/j.jwpe.2021.101954.

[29] L.M. Pandey, Surface engineering of nano-sorbents for the removal of heavy metals: Interfacial aspects, J. Environ. Chem. Eng. 9 (2021) 104586. https://doi.org/https://doi.org/10.1016/j.jece.2020.104586.

[30] K. Rambabu, A. Avornyo, T. Gomathi, A. Thanigaivelan, P.L. Show, F. Banat, Phycoremediation for carbon neutrality and circular economy: Potential, trends, and challenges, Bioresour. Technol. 367 (2023) 128257. https://doi.org/10.1016/j.biortech.2022.128257.

[31] V. Arya, L. Philip, Adsorption of pharmaceuticals in water using Fe3O4 coated polymer clay composite, Microporous Mesoporous Mater. 232 (2016) 273–280. https://doi.org/https://doi.org/10.1016/j.micromeso.2016.06.033.

[32] S. Ravi, Y. Choi, J.K. Choe, Novel phenyl-phosphate-based porous organic polymers

for removal of pharmaceutical contaminants in water, Chem. Eng. J. 379 (2020) 122290. https://doi.org/https://doi.org/10.1016/j.cej.2019.122290.

[33] A. Zeraatkar Moghaddam, E. Ghiamati, A. Ayati, M.R. Ganjali, Application of the response surface methodology for optimizing the adsorptive removal of chromate using a magnetic crosslinked chitosan nanocomposite, J. Appl. Polym. Sci. 136 (2019) 47077. https://doi.org/https://doi.org/10.1002/app.47077.

[34] B. Tanhaei, A. Ayati, E. Iakovleva, M. Sillanpää, Efficient carbon interlayed magnetic chitosan adsorbent for anionic dye removal: Synthesis, characterization and adsorption study, Int. J. Biol. Macromol. 164 (2020) 3621–3631. https://doi.org/https://doi.org/10.1016/j.ijbiomac.2020.08.207.

[35] A. Bhatnagar, M. Sillanpää, Applications of chitin- and chitosan-derivatives for the detoxification of water and wastewater — A short review, Adv. Colloid Interface Sci. 152 (2009) 26–38. https://doi.org/https://doi.org/10.1016/j.cis.2009.09.003.

[36] Z. Shariatinia, Carboxymethyl chitosan: Properties and biomedical applications, Int. J. Biol. Macromol. 120 (2018) 1406–1419. https://doi.org/https://doi.org/10.1016/j.ijbiomac.2018.09.131.

[37] P. Miretzky, A.F. Cirelli, Fluoride removal from water by chitosan derivatives and composites: A review, J. Fluor. Chem. 132 (2011) 231–240. https://doi.org/https://doi.org/10.1016/j.jfluchem.2011.02.001.

[38] M.S. Sivakami, T. Gomathi, J. Venkatesan, H.S. Jeong, S.K. Kim, P.N. Sudha, Preparation and characterization of nano chitosan for treatment wastewaters, Int. J. Biol. Macromol. 57 (2013) 204–212. https://doi.org/10.1016/j.ijbiomac.2013.03.005.

[39] L. Qi, Z. Xu, Lead sorption from aqueous solutions on chitosan nanoparticles, Colloids Surfaces A Physicochem. Eng. Asp. 251 (2004) 183–190.

https://doi.org/https://doi.org/10.1016/j.colsurfa.2004.10.010.

[40] M. Nasrollahzadeh, M. Sajjadi, S. Iravani, R.S. Varma, Starch, cellulose, pectin, gum, alginate, chitin and chitosan derived (nano)materials for sustainable water treatment: A review, Carbohydr. Polym. 251 (2021) 116986. https://doi.org/https://doi.org/10.1016/j.carbpol.2020.116986.

[41] C. Xu, M. Nasrollahzadeh, M. Sajjadi, M. Maham, R. Luque, A.R. Puente-Santiago, Benign-by-design nature-inspired nanosystems in biofuels production and catalytic applications, Renew. Sustain. Energy Rev. 112 (2019) 195–252. https://doi.org/https://doi.org/10.1016/j.rser.2019.03.062.

[42] B. An, H. Lee, S. Lee, S.-H. Lee, J.-W. Choi, Determining the selectivity of divalent metal cations for the carboxyl group of alginate hydrogel beads during competitive sorption, J. Hazard. Mater. 298 (2015) 11–18. https://doi.org/https://doi.org/10.1016/j.jhazmat.2015.05.005.

[43] Y. Kuang, J. Du, R. Zhou, Z. Chen, M. Megharaj, R. Naidu, Calcium alginate encapsulated Ni/Fe nanoparticles beads for simultaneous removal of Cu (II) and monochlorobenzene, J. Colloid Interface Sci. 447 (2015) 85–91. https://doi.org/https://doi.org/10.1016/j.jcis.2015.01.080.

[44] R. Ahmad, A. Mirza, Sequestration of heavy metal ions by Methionine modified bentonite/Alginate (Meth-bent/Alg): A bionanocomposite, Groundw. Sustain. Dev. 1 (2015) 50–58. https://doi.org/https://doi.org/10.1016/j.gsd.2015.11.003.

[45] S. George, D. Mehta, V.K. Saharan, Application of hydroxyapatite and its modified forms as adsorbents for water defluoridation: an insight into process synthesis, Rev Chem Eng. 36 (2020) 369–400. https://doi.org/doi:10.1515/revce-2017-0101.

[46] G. Ciobanu, M. Harja, L. Rusu, A.M. Mocanu, C. Luca, Acid Black 172 dye

adsorption from aqueous solution by hydroxyapatite as low-cost adsorbent, Korean J. Chem. Eng. 31 (2014) 1021–1027. https://doi.org/10.1007/s11814-014-0040-4.

[47] D. Ghahremani, I. Mobasherpour, E. Salahi, M. Ebrahimi, S. Manafi, L. Keramatpour, Potential of nano crystalline calcium hydroxyapatite for Tin(II) removal from aqueous solutions: Equilibria and kinetic processes, Arab. J. Chem. 10 (2017) S461–S471. https://doi.org/https://doi.org/10.1016/j.arabjc.2012.10.006.

[48] H. Tanaka, M. Futaoka, R. Hino, K. Kandori, T. Ishikawa, Structure of synthetic calcium hydroxyapatite particles modified with pyrophosphoric acid, J. Colloid Interface Sci. 283 (2005) 609–612. https://doi.org/https://doi.org/10.1016/j.jcis.2004.09.013.

[49] A.N. Amenaghawon, C.L. Anyalewechi, H. Darmokoesoemo, H.S. Kusuma, Hydroxyapatite-based adsorbents: Applications in sequestering heavy metals and dyes, J. Environ. Manage. 302 (2022) 113989. https://doi.org/10.1016/j.jenvman.2021.113989.

[50] K. Vijayalakshmi, T. Gomathi, S. Latha, T. Hajeeth, P.N. Sudha, Removal of copper(II) from aqueous solution using nanochitosan/sodium alginate/microcrystalline cellulose beads, Int. J. Biol. Macromol. 82 (2016) 440–452. https://doi.org/10.1016/j.ijbiomac.2015.09.070.

[51] S. Pavithra, T. Gomathi, S. S, S. P.N., H.H. Alkhamis, A.F. Alrefaei, M.H. Almutairi, Batch adsorption studies on surface tailored chitosan/orange peel hydrogel composite for the removal of Cr(VI) and Cu(II) ions from synthetic wastewater, Chemosphere. 271 (2021) 129415. https://doi.org/10.1016/j.chemosphere.2020.129415.

[52] T. Gomathi, P. Supriya Prasad, P.N. Sudha, A. Sukumaran, Size optimization and in vitro biocompatibility studies of chitosan nanoparticles, Int. J. Biol. Macromol. 104

(2017) 1794–1806. https://doi.org/10.1016/j.ijbiomac.2017.08.057.

[53] S. Sugashini, T. Gomathi, S. Pavithra, P.N. Sudha, J.A.K. Florence, A. Mubashirunnisa, Removal of Copper(II) Ion using Nanochitosan/Carboxymethyl Cellulose/Grapheme Oxide Composite Biosorbent, Asian J. Chem. 34 (2022) 1465–1471.

[54] A.M. Omer, R.E. Khalifa, Z. Hu, H. Zhang, C. Liu, X. Ouyang, Fabrication of tetraethylenepentamine functionalized alginate beads for adsorptive removal of Cr (VI) from aqueous solutions, Int. J. Biol. Macromol. 125 (2019) 1221–1231. https://doi.org/https://doi.org/10.1016/j.ijbiomac.2018.09.097.

[55] R. Yi, W. Cai, C. Dang, B. Han, L. Liu, J. Fan, Mild hydrothermal preparation of millimeter-sized carbon beads from chitosan with significantly improved adsorption stability for Cr(VI), Chem. Eng. Res. Des. 156 (2020) 43–53. https://doi.org/https://doi.org/10.1016/j.cherd.2020.01.026.

[56] R.M. Vieira, P.B. Vilela, V.A. Becegato, A.T. Paulino, Chitosan-based hydrogel and chitosan/acid-activated montmorillonite composite hydrogel for the adsorption and removal of Pb+2 and Ni+2 ions accommodated in aqueous solutions, J. Environ. Chem. Eng. 6 (2018) 2713–2723. https://doi.org/https://doi.org/10.1016/j.jece.2018.04.018.

[57] A.M. Omer, R. Dey, A.S. Eltaweil, E.M. Abd El-Monaem, Z.M. Ziora, Insights into recent advances of chitosan-based adsorbents for sustainable removal of heavy metals and anions, Arab. J. Chem. 15 (2022) 103543. https://doi.org/https://doi.org/10.1016/j.arabjc.2021.103543.

[58] J.D. Cuppett, S.E. Duncan, A.M. Dietrich, Evaluation of Copper Speciation and Water Quality Factors That Affect Aqueous Copper Tasting Response, Chem. Senses. 31

(2006) 689–697. https://doi.org/10.1093/chemse/bjl010.

[59] M.R. Gopal Reddi, T. Gomathi, M. Saranya, P.N. Sudha, Adsorption and kinetic studies on the removal of chromium and copper onto Chitosan-g-maliec anhydride-g-ethylene dimethacrylate, Int. J. Biol. Macromol. 104 (2017) 1578–1585. https://doi.org/10.1016/j.ijbiomac.2017.01.142.

[60] T.N. Balaji, S.M.A. Rahman, T. Gomathi, P.N. Sudha, A.K.S.I. Sheriff, Crosslinked chitosan oligosaccharide-based binary and ternary blends for the removal of Cu(II) ions, Int. J. Environ. Sci. Technol. (2021). https://doi.org/10.1007/s13762-021-03704-5.

[61] J.T. Bamgbose, S. Adewuyi, O. Bamgbose, A.A. Adetoye, Adsorption kinetics of cadmium and lead by chitosan, African J. Biotechnol. 9 (2010) 2560–2565.

[62] V. Vadivelan, K.V. Kumar, Equilibrium, kinetics, mechanism, and process design for the sorption of methylene blue onto rice husk, J. Colloid Interface Sci. 286 (2005) 90–100. https://doi.org/https://doi.org/10.1016/j.jcis.2005.01.007.

[63] K. Kadirvelu, C. Namasivayam, Agricutural By-Product as Metal Adsorbent: Sorption of Lead(II) from Aqueous Solution onto Coirpith Carbon, Environ. Technol. 21 (2000) 1091–1097. https://doi.org/10.1080/09593330.2000.9618995.

[64] A. Akgerman, M. Zardkoohi, Adsorption of phenolic compounds on fly ash, J. Chem. \& Eng. Data. 41 (1996) 185–187.

[65] R.-S. Juang, R.-L. Tseng, F.-C. Wu, Role of Microporosity of Activated Carbons on Their Adsorption Abilities for Phenols and Dyes, Adsorption. 7 (2001) 65–72. https://doi.org/10.1023/A:1011225001324.

Dr. Yabesh Abraham Durairaj Isravel, “Analysis of Ethical Aspects Among Bank Employees with Relation to Job Stratification Level” Eur. Chem. Bull. 2023, 12(Special Issue 4),

3970-3976.

[66] V.K. Gupta, R. Jain, S. Malathi, A. Nayak, Adsorption–desorption studies of indigocarmine from industrial effluents by using deoiled mustard and its comparison with charcoal, J. Colloid Interface Sci. 348 (2010) 628–633. https://doi.org/https://doi.org/10.1016/j.jcis.2010.04.085.

[67] V.K. Gupta, A. Rastogi, Equilibrium and kinetic modelling of cadmium(II) biosorption by nonliving algal biomass Oedogonium sp. from aqueous phase, J. Hazard. Mater. 153 (2008) 759–766. https://doi.org/https://doi.org/10.1016/j.jhazmat.2007.09.021.

[68] E. Bulut, M. Özacar, İ.A. Şengil, Equilibrium and kinetic data and process design for adsorption of Congo Red onto bentonite, J. Hazard. Mater. 154 (2008) 613–622. https://doi.org/https://doi.org/10.1016/j.jhazmat.2007.10.071.

[69] Y. Nuhoglu, E. Malkoc, Thermodynamic and kinetic studies for environmentaly friendly Ni(II) biosorption using waste pomace of olive oil factory., Bioresour. Technol. 100 (2009) 2375–2380. https://doi.org/10.1016/j.biortech.2008.11.016.

[70] Y.N. Mata, M.L. Blázquez, A. Ballester, F. González, J.A. Muñoz, Biosorption of cadmium, lead and copper with calcium alginate xerogels and immobilized Fucus vesiculosus, J. Hazard. Mater. 163 (2009) 555–562. https://doi.org/https://doi.org/10.1016/j.jhazmat.2008.07.015.